Dynamics of motor-related functional integration during motor sequence learning

David Coynel [a,b,c,*], Guillaume Marrelec [a,b,c], Vincent Perlbarg [a,b,c], Mélanie Pélégrini-Issac [a,b,c], Pierre-François Van de Moortele [d], Kamil Ugurbil [d], Julien Doyon [a,c,e], Habib Benali [a,b,c,e], Stéphane Lehéricy [b,c,d,f]

[a] Inserm and UPMC Univ Paris 06, UMR-S 678 Laboratoire d'Imagerie Fonctionnelle, Paris, F-75013 Paris, France
[b] IFR49-Institut Fédératif d'Imagerie Neurofonctionnelle, Gif-Sur-Yvette, F-91191, France
[c] Inserm, University of Montreal, and UPMC Univ Paris 06, Laboratoire International de Neuroimagerie et Modélisation (LINeM), France
[d] University of Minnesota, CMRR/Department of Radiology, Minneapolis, USA
[e] University of Montreal, Geriatric Institute, UNF, Montreal Canada H3W 1W5
[f] UPMC Univ Paris 06, Centre de NeuroImagerie de Recherche-CENIR, CHU Pitié-Salpêtrière, Paris, F-75013, France

ARTICLE INFO

ABSTRACT

Motor skill learning is associated with profound changes in brain activation patterns over time. Associative and rostral premotor cortical and subcortical regions are mostly recruited during the early phase of explicit motor learning, while sensorimotor regions may increase their activity during the late learning phases. Distinct brain networks are therefore engaged during the early and late phases of motor skill learning. How these regions interact with one another and how information is transferred from one circuit to the other has been less extensively studied. In this study, we used functional MRI (fMRI) at 3T to follow the changes in functional connectivity in the associative/premotor and the sensorimotor networks, during extended practice (4 weeks) of an explicitly known sequence of finger movements. Evolution of functional connectivity was assessed using integration, a measure that quantifies the total amount of interaction within a network. When comparing the integration associated with a complex finger movement sequence to that associated with a simple sequence, we observed two patterns of decrease during the 4 weeks of practice. One was not specific as it was observed for all sequences, whereas a specific decrease was observed only for the execution of the learned sequence. This second decrease was a consequence of a relative decrease in associative/premotor network integration, together with a relative increase in between-network integration. These findings are in line with the hypothesis that information is transferred from the associative/premotor circuit to the sensorimotor circuit during the course of motor learning.

© 2009 Elsevier Inc. All rights reserved.

Introduction

Motor skill learning is associated with profound changes in brain activation patterns over time. During the early phase of explicit motor learning, associative frontal regions including the dorsolateral prefrontal cortex (DLPFC) and rostral premotor areas, as well as associative basal ganglia and cerebellum are mostly recruited (Floyer-Lea and Matthews, 2005; Tamás Kincses et al., 2008; Doyon et al., 2009). They show greater activity at the beginning of learning. Furthermore, some areas show increased activation during later phases of motor sequence learning, such as the sensorimotor territory of the basal ganglia and the cerebellar dentate nucleus (Doyon et al., 2002; Lehéricy et al., 2005). These data suggest that distinct cerebellar–basal ganglia–cortical networks are engaged during the early and late phases of motor skill learning. How these regions interact with one another and how infor-

mation is transferred from one circuit to the other has been less extensively studied.

However, models of brain dynamics of motor skill learning have been proposed (Hikosaka et al., 2002). According to this model, a sequence of movements is represented in two different coordinate systems, spatial and motor. At the beginning of learning, movements are executed individually through associative frontoparietal regions and associative regions of the basal ganglia and cerebellum and encoded in spatial coordinates. During learning, the movement sequence is gradually built up in motor coordinates in the sensorimotor loop circuit that includes motor-related cortical areas and motor territories of the basal ganglia and cerebellum. This model also postulates that the coordinate transformation process is achieved through intracortical connections from the association cortices to the motor cortices. Therefore, dynamic interactions between these neural networks appear to be an essential feature of motor skill learning. Characterization of the dynamic interactions of these networks is essential to the understanding of motor skill learning. Here we used functional MRI (fMRI) at 3T to follow the changes in the time course of functional connectivity in the associative and motor networks during

---

* Corresponding author. Inserm and UPMC Univ Paris 06, UMR-S 678 Laboratoire d'Imagerie Fonctionnelle, CHU Pitié-Salpêtrière, 91 Boulevard de l'Hôpital, F-75013 Paris, France. Fax: +33 153 828 448.
E-mail address: david.coynel@imed.jussieu.fr (D. Coynel).

4 weeks of practice of an explicitly known sequence of finger movements. Functional networks involved in the early and late phases of learning were identified using an approach based on spatial independent component analysis (sICA) (Perlbarg et al., 2008). Functional connectivity within and between these networks was assessed using a measure called hierarchical integration (Marrelec et al., 2008) that gives access to information exchanges within a network, and between networks.

Materials and methods

The results presented in this study constitute a re-analysis of a previously published study (Lehéricy et al., 2005), using new analytical tools. We provide relevant information about the participants, task and scanning parameters. For more details concerning the original study, readers are referred to Lehéricy et al. (2005).

Subjects

Twelve volunteers participated in the present study (6 men, mean age = 23.5 ± 4.3 years, age range: 19–34 years). None of the subjects was a musician or a professional typist. One subject had previously played the piano, but stopped practicing more than 7 years before. The Local Ethics Committee from the University of Minnesota approved the study, and the subjects gave their informed consent. All subjects were-right handed as confirmed by the Edinburgh Handedness Inventory.

Motor task

The motor learning protocol was extensively detailed previously (Lehéricy et al., 2005). Briefly, subjects had to practice 10 to 20 minutes daily during 4 weeks a sequence of eight digits using fingers 2 (index finger) to 5 (little finger) of the left hand. The sequences were generated using MATLAB® (The Mathworks Inc., Natick, MA, USA). Within each sequence, the order of finger movements was pseudo-randomly generated such that each finger was used twice in each sequence. For each subject, one sequence was randomly chosen to be the trained sequence (T-sequence), while three other sequences (one for each fMRI session) served as untrained new sequences (U-sequences). A third simple sequence (2–3–4–5–2–3–4–5), where no learning was expected, was also used as a control overlearned sequence (C-sequence). One fMRI session was performed on day 1. Two additional sessions were also carried out after 14 and 28 days of practice, respectively. During each fMRI session, subjects had to perform 3 runs: the T-sequence, the U-sequence (which differed at each session), and the C-sequence. Each run consisted of ten alternated epochs of 27 s of rest and 27 s of the motor condition. The order of the runs was counterbalanced across subjects. Movements were audio-paced with computer generated sounds at a frequency of 2 Hz.

Imaging protocol

The MR protocol was carried out with a 3T whole-body system (Siemens, Erlangen, Germany) at the Center for Magnetic Resonance Research/Department of Radiology, University of Minnesota, Minneapolis. Blood oxygen level-dependent (BOLD) fMRI signal was used. For each run, whole brain coverage was obtained with 43 oblique axial gradient echo echo-planar imaging (EPI) images (repetition time TR = 4.5 s; echo time TE = 40 ms; α = 90°; bandwidth 1.562 Hz per pixel; field of view FOV 192 × 192 mm²; voxel size 1.5 × 1.5 × 2.5 mm³; partial Fourier imaging 6/8). Each run consisted of 123 EPI volumes. Subsequently, a high-resolution structural volume was acquired using a 3D magnetization prepared rapid gradient echo (MP-RAGE) sequence (144 sagittal images; thickness 1 mm; FOV 256 × 256 mm²; matrix size 256 × 256).

fMRI data analysis

Pre-processing

K-space functional data were processed to reduce physiological noise using a retrospective estimation and correction of respiration and heart beat (Hu et al., 1995). The first two and the last volumes were discarded for signal stabilization. A temporal cut-off (cutoff frequency $4.16 × 10^{-3}$ Hz) was applied to the functional data to filter out subject-specific low-frequency drifts of the signal. Data were then corrected for subject's motion, with the first volume of each run as a reference, and resliced using 4th degree B-Spline interpolation with the SPM2[1] software. Finally, the same software was used to smooth the images with an isotropic Gaussian spatial filter of full-width-at-half-maximum 5 mm.

Regions of interest selection

Our objective was to quantify functional connectivity within the motor sequence learning (MSL) network along the motor learning process. Definition of regions of interest (ROIs) belonging to the MSL motor network was based on a motor skill learning model, which gives priors on the brain regions involved (Hikosaka et al., 2002). However precise anatomical location (e.g. Talairach-space coordinates) of these regions was not available in the model. We consequently started the fMRI analysis by applying an exploratory method, based on spatial independent component analysis (sICA, Perlbarg et al. (2008)), to extract group representative functional large-scale networks. Among these networks obtained in a data-driven way, we identified the MSL network as the one that comprised the regions mentioned in Hikosaka's model, and anatomically localized ROIs on the corresponding spatial maps.

Spatial ICA analysis was carried out for each session (days 1, 14, or 28) and each run (T-, U-, C-sequences). This method can be broken down into three steps. First, the 40 spatial components explaining the most variance were extracted for each subject and each run, using an infomax ICA algorithm. These components were scaled to z-scores and registered to the Montreal Neurological Institute (MNI) standard space using nonlinear spatial transformations as implemented in SPM2. The second step consisted of clustering independent components across subjects for each run, based on their spatial similarity (Esposito et al., 2005). Finally, partitioning of the hierarchy was automatically performed for each run, using criteria optimizing both the unicity and the representativity of each extracted class. The representativity criterion controls that each subject is represented with at least one component in a given class, whereas the unicity criterion controls that a subject contributes to a class with one and only one component. These criteria have values between 0 and 1, and an optimal class is characterized by a value of 1 for both representativity and unicity. For each of the resulting group-representative classes, a fixed-effect group map of t-scores was computed, corrected for false discovery rate (FDR) and thresholded at $p \leq 0.05$.

Within this set of group-representative maps exhibiting spatially structured functional processes and noise processes, we visually identified the one exhibiting a spatial organization distributed into cortical, sub-cortical, and cerebellar areas corresponding to the regions defined in the motor skill learning model (Hikosaka et al., 2002). This map was identified for each run, and its representativity and unicity were both 1. Furthermore, the time course associated to this map corresponded to the alternating task/rest design of the motor task.

According to the motor skill learning model by Hikosaka et al. (2002), we then defined the MSL network, comprising two subnetworks: the associative/premotor (AP) network and the sensorimotor (SM) network. The AP network was derived from the motor-task spatial map of the T-sequence run on day 1. The SM network was derived from

---

[1] Wellcome Department of Cognitive Neurology, London, UK - http://www.fil.ion.ucl.ac.uk/spm/software/spm2/.

the motor-task spatial map of the T-sequence run on day 28. Regions of interest belonging to each of the two subnetworks were defined following the model by Hikosaka et al. (2002), using anatomical atlas priors and according to the *t*-score distribution of the subnetworks' spatial map. For cortical and cerebellar ROIs, we used the automated anatomical parcellation of the MNI single-subject T1-weighted MRI (Tzourio-Mazoyer et al., 2002). For sub-cortical ROIs, we used a post-mortem three-dimensional deformable atlas of the basal ganglia (Yelnik et al., 2007). This single-subject atlas was coregistered to the MNI standard space using nonlinear spatial transformations as implemented in SPM2. Associative and sensorimotor subdivisions of the putamen were considered. The ventral anterior (VA) nucleus was associated with the associative territory of the thalamus, and the ventral lateral (VL) and ventralis intermedius (VIM) nuclei were associated with the sensori-motor territory (Alexander et al., 1986; Romanelli et al., 2005; Lehéricy et al., 2006).

The AP network was then composed of 10 ROIs, and the SM network of 7 ROIs. ROIs of the AP network included bilateral pre-SMA, bilateral premotor cortices, the left inferior parietal cortex (BA40), bilateral cerebellar hemispheres (lateral parts of lobule VI), putamen and thalamus. ROIs of the SM network included the SMA, the right sensorimotor cortex, lobule IV–V of the cerebellum, bilateral putamen and bilateral thalamus (Table 1). For each network, seed voxels were chosen for each ROI as the voxel with the maximum local *t*-score in the corresponding MSL map. From these seed voxels, ROIs were obtained based on a local maximum search algorithm: first, an adjacency matrix of the voxels belonging to the spatial map was built. Among all neighboring voxels, the one with the highest *t*-score was included in the ROI. This process was repeated with the new ROI and its neighboring voxels, until a given size was reached, which was adapted to the size of the underlying anatomical structure (200 voxels, 1120 mm³—for cortical and cerebellar regions, 100 voxels, 560 mm³—for putaminal regions and 50 voxels, 280 mm³—for thalamic regions).

To compare the spatial organization of the motor-task networks along the training process and for the three different sequences, we used a measure of spatial similarity in order to create a distance matrix **D** between all the maps. Multidimensional scaling (MDS) analysis (Mardia et al., 1979) was then used to plot the best approximation $\hat{\mathbf{D}}$ of **D** in a two-dimensional Euclidean space. Maps with a similar spatial organization are close to each other in this representation.

Hierarchical integration

Background. Information theory was originally developed in the 1950s by Shannon, to better characterize communicating systems and noisy channels (Shannon, 1948). In particular, he introduced a key quantity: entropy, which measures the information contained in a message. Since then, this measure has been widely applied to several fields, including neurosciences. Indeed, coherent behavior and cognition are known to emerge through the integration of information flows between segregated regions, organized into large-scale networks (Varela et al., 2001). Consequently, measures characterizing inter-actions within and between these networks are essential to the understanding of brain function. In this paper we applied a measure deriving from entropy, hierarchical integration, which is aimed at quantifying information exchanges between and within networks involved in motor sequence learning.

Definition. Functional connectivity is classically defined as the temporal correlation between regions' time courses (Friston, 1994). Since the MSL network is composed of 17 regions, functional connectivity within this network is fully characterized by all the correlation coefficients that can be computed from these 17 regions, i.e., the $17 \times (17 - 1) / 2 = 136$ coefficients that form the correlation matrix **R**. In order to quantify the global change in functional connectivity induced by learning, we resorted to a measure known as total correlation in information theory (Watanabe, 1960) and integration in neurocomputing (Tononi et al., 1994). If $\boldsymbol{\Sigma}$ is the model covariance matrix, integration of the MSL network can be defined as (Marrelec et al., 2008):

$$I_{\mathrm{MSL}} = \frac{1}{2}\ln\left[\frac{\prod_{i=1}^{17}\Sigma_{ii}}{|\boldsymbol{\Sigma}|}\right], \tag{1}$$

where $|\cdot|$ stands for the determinant. It can be shown that I_{MSL} can also be expressed as a function of **R** as

$$I_{\mathrm{MSL}} = -\frac{1}{2}\ln|\mathbf{R}|. \tag{2}$$

This expression shows that integration derives from functional connectivity, summarizing the 136 correlation coefficients in one

Table 1
Regions of interest MNI coordinates.

Region	Peak label (AAL or Basal Ganglia)	Peak t-score	Peak MNI coordinates		
			x	Y	z
AP regions					
Pre-SMA	Supplementary motor area	17.2	1.5	4.5	50
Premotor cortex (R)	Precentral	18.0	28.5	−7.5	57.5
Premotor cortex (L)	Precentral	11	−31.5	−13.5	65
Parietal cortex (L)	Parietal inferior	16.9	−34.5	−43.5	47.5
Cerebellum (R)	Cerebellum VI	17.2	37.5	−55.5	−27.5
Cerebellum (L)	Cerebellum VI	22.7	−25.5	−55.5	−27.5
Putamen (R)	Associative	21.5	28.5	4.5	0
Putamen (L)	Associative	15.4	−22.5	0	5
Thalamus (R)	Ventral anterior	18.2	12	−15	0
Thalamus (L)	Ventral anterior	9.8	−7.5	−15	0
SM regions					
SMA	Supplementary motor area	19.8	−1.5	−7.5	62.5
Sensorimotor cortex (R)	Postcentral	46.4	37.5	−22.5	50
Cerebellum (L)	Cerebellum IV–V	16.4	−16.5	−51	−25
Putamen (R)	Sensorimotor	10.6	31.5	−7.5	−2.5
Putamen (L)	Sensorimotor	7.8	−22.5	−4.5	5
Thalamus (R)	Ventral lateral	10.9	16.5	−16.5	5
Thalamus (L)	Ventralis intermedius	6.1	−12	−19.5	5

MNI coordinates of the seed voxels for the premotor/associative (AP) and the sensorimotor (SM) networks. *t*-scores are extracted from the thresholded ($p \leq 0.05$), FDR corrected group-representative maps of the T-sequence run on Day 1 (AP network) and 28 (SM network). Peak labels are given according to the two atlases : the automated anatomical labeling (AAL, Tzourio-Mazoyer et al. (2002)) for cortical and cerebellar seeds, and the three-dimensional atlas of the human basal ganglia (Yelnik et al., 2007) for putaminal and thalamic seeds.

single number. When all correlation coefficients are equal to zero (i.e., there is no functional connectivity), integration is also equal to zero; otherwise, it is positive. The larger the correlation coefficients, the larger the integration.

Integration was also used to quantify functional connectivity within subnetworks AP and SM. We then decomposed the covariance matrix as: $\Sigma = \begin{bmatrix} \Sigma_{AP,AP} & \Sigma_{AP,SM} \\ \Sigma_{SM,AP} & \Sigma_{SM,SM} \end{bmatrix}$. In a fashion similar to Eq. 1, integration for these subnetworks then reads

$$I_{AP} = \frac{1}{2}\ln\left[\frac{\Pi_{i\in AP}\Sigma_{ii}}{|\Sigma_{AP,AP}|}\right]$$

and

$$I_{SM} = \frac{1}{2}\ln\left[\frac{\Pi_{i\in SM}\Sigma_{ii}}{|\Sigma_{SM,SM}|}\right].$$

Now, according to the hierarchical feature of integration (Marrelec et al., 2008), integrations of the MSL, AP, and SM networks are related by

$$I_{MSL} = I_{AP} + I_{SM} + I_{AP/SM}, \tag{3}$$

where we set $I_{AP/SM} = \frac{1}{2}\ln\left[\frac{|\Sigma_{AP,AP}|\cdot|\Sigma_{SM,SM}|}{|\Sigma|}\right]$.

$I_{AP/SM}$ can be interpreted as a quantification of functional connectivity between subnetworks AP and SM. The above relationship then states that the integration of network MSL can be decomposed into the sum of the integration measured within each subnetwork AP or SM, and an integration term quantifying between-subnetworks functional connectivity.

To study the relative contributions of each system, as well as the between-system integrations, to the total integration, we computed the following quantities: $I_{AP}^R = \frac{I_{AP}}{I_{MSL}}$, $I_{SM}^R = \frac{I_{SM}}{I_{MSL}}$, and $I_{AP/SM}^R = \frac{I_{AP/SM}}{I_{MSL}}$. These values measure the amount of integration allocated to a system, relatively to the amount of available total (MSL) integration. They represent percentages of variations and, according to Eq. (3), they vary between 0 and 1.

Bayesian inference. The parameter Σ of the Gaussian model is necessary to calculate integration. Since it is unknown and only partly accessible through the data, the values of integration were inferred using a Bayesian numerical sampling scheme that approximated the posterior distribution of the parameters of interest in a group analysis (Marrelec et al., 2006). A mean value and a standard deviation for each value of integration $I_{system, time, sequence}$ (time = days 1, 14, or 28; sequence = T, U, or C) were then computed from this sampling scheme.
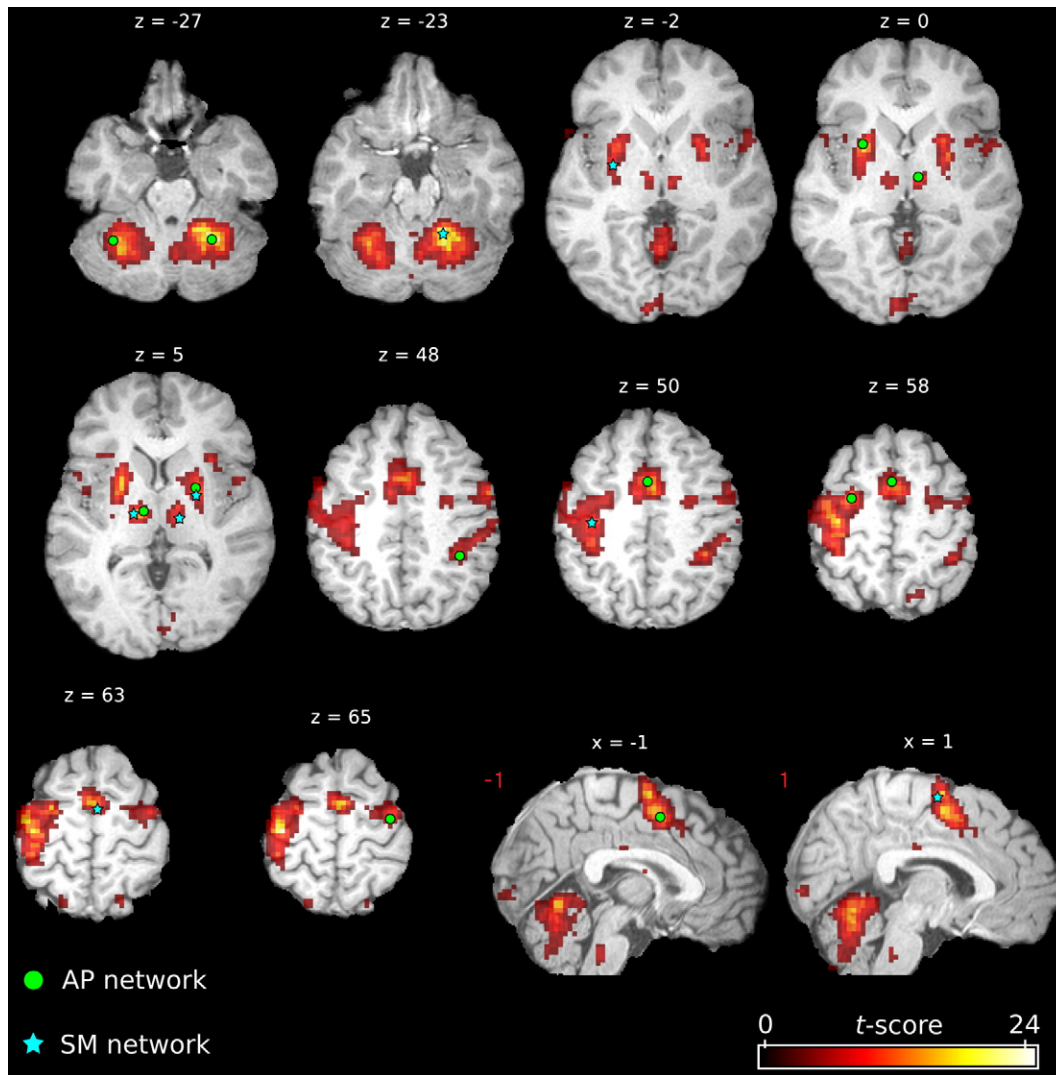
Fig. 1. Seed voxels for the regions of interest of the associative/premotor (AP, green dots) and sensorimotor (SM, blue stars) networks. The seeds are displayed on the thresholded ($p<0.05$), FDR corrected t-score motor-task map of the trained sequence on day 1, surimposed on an anatomical template in the MNI standard space (MNI512). Images are shown in radiological convention (i.e., image left side corresponds to subject's right side).
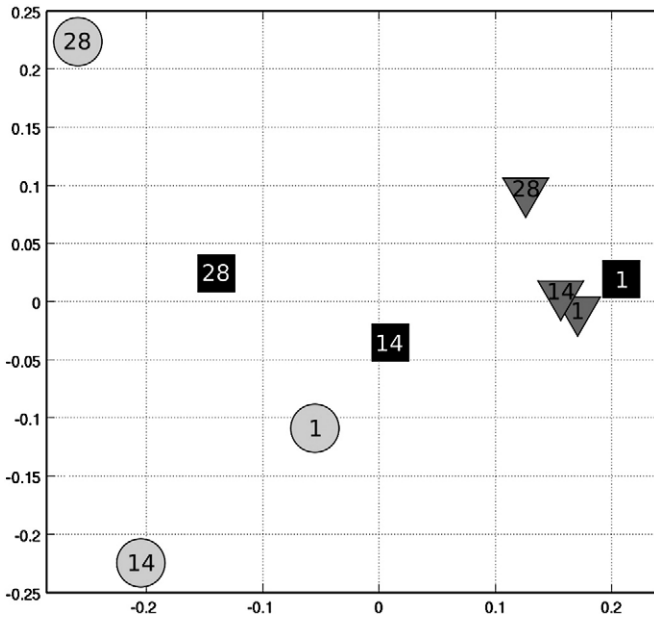
Fig. 2. Multidimensional scaling of the spatial maps of the motor-task networks on days 1, 14 and 28 for the trained (squares), untrained (triangles), and control (circles) sequences. Axes represent the Euclidian distance between maps.

$N = 5000$ integration values were computed from the sampling scheme, from which statistics can be obtained. It was in particular possible to approximate the posterior probability $p(A|\mathbf{y})$ of an assertion A related to any pair of integration measure (I_{MSL}, I_{AP}^R, I_{SM}^R, $I_{AP/SM}^R$), given the ROIs' BOLD fMRI time courses ($\mathbf{y}$). A can represent any assertion that has to be tested, but we chose to make only pairwise comparisons. For example, to test if on day 14 the integration value of the trained sequence was lower than the integration value of the untrained sequence, in the MSL network, the assertion A was defined as: $A = "I_{MSL,\,14,\,T} < I_{MSL,\,14,\,U}"$ and its posterior probability as

$$p(A|\mathbf{y}) \approx \frac{1}{N} \# \left\{ i : I_{MSL,\,14,\,T}^{[i]} < I_{MSL,\,14,\,U}^{[i]} \right\},$$

where $i = (1, …, N)$, and # stands for the cardinal function of a set. The validity of the assertion could then be tested using a measure called evidence (Jaynes, 2003):

$$e(A|\mathbf{y}) = 10\log_{10}\left[\frac{p(A|\mathbf{y})}{1 - p(A|\mathbf{y})}\right],$$

measured in decibels (dB). What we actually study with evidence is then the ratio of the probability that A is true to the probability that A is false, in a base 10 logarithmic scale. According to this measure, two values of integration will be said significantly different when $|e(A|\mathbf{y})| > 10$ dB, which corresponds to a ratio $\frac{p(A|\mathbf{y})}{1-p(A|\mathbf{y})}$ higher than 10:1. In other words, a probability of A being true $p(A|\mathbf{y}) > 0.909$. To correctly interpret this measure, it should be noted that a significant positive value of evidence shows that the assertion A is true, but, on the other hand, a significant negative value shows that the complementary assertion $\bar{A}$ has to be considered as true. In the previous example it would be: $\bar{A} = "I_{MSL,\,14,\,T} \geq I_{MSL,\,14,\,U}"$.

Results

Spatial maps

Regions of interest

Regions of interest selected for the study, as described in the methods, are shown on the group-representative motor-task spatial map of the T-run sequence on day 1 (Fig. 1).

Multidimensional scaling

Multidimensional scaling was used to compute a plane that best represented the distance matrix **D** between the spatial maps of the motor-task networks for the different conditions. It showed an evolution of the motor networks along the training process (Fig. 2). Maps of the U-sequence remained identical: there was little variation of their representation on both axes. On the other hand, maps of the T-sequence evolved mainly on the x-axis, being similar to the U-sequence on day 1, and similar to the C-sequence on day 28. Maps of the C-sequence also varied on both axes but remained clearly separated from maps of the U-sequence.

Hierarchical integration

We computed the level of hierarchical integration of the MSL, AP/SM, and SM networks for the three runs of the T, U, and C-sequences. Statistical tests were conducted using assertions such as: $A = "Is\ I_{MSL,\,14,\,T} < I_{MSL,\,14,\,U}"$ to test for the difference between pairs of integration values. Results are given as evidence values e in Table 2. Values of I_{MSL}, I_{AP}^R, I_{SM}^R, and $I_{AP/SM}^R$ are presented in Fig. 3.

Motor sequence learning network integration (I_{MSL})

On day 1, integrations of the MSL network for the T and U-sequences did not differ ($|e| = 6.25$), and were significantly higher than the integration value of the C-sequence. On day 14, all integration values differed significantly, with integration of the T-sequence being significantly lower than the U-sequence and higher than the C-sequence. On day 28, integrations of the MSL network for the T and C-sequences did not differ ($|e| = 0.35$), and were significantly smaller than the integration value of the U-sequence.

Relative AP/SM integration ($I_{AP/SM}^R$)

On day 1, integrations of the T and U-sequences did not differ ($|e| = 5.53$), and were smaller than the integration value of the C-sequence. On day 14, however, all integration values differed significantly, with integration of the T-sequence being significantly higher than the U-sequence and lower than the C-sequence. On day 28, integrations of the T and C-sequences did not differ ($|e| = 5.43$), and were significantly higher than the integration value of the U-sequence.

Relative AP network integration (I_{AP}^R)

We observed the same pattern for the relative integration of the AP network as for the MSL network. On day 1, integrations of the T- and U-sequences did not differ ($|e| = 8.33$), and both values were higher than

Table 2
Evidence values.

	$T < U$	$C < T$	$C < U$
I_{MSL}			
Day 1	−6.25	**36.99**	**21.65**
Day 14	**36.99**	**19.38**	**>40.0**
Day 28	**30.97**	−0.35	**30.97**
$I_{AP/SM}^R$			
Day 1	5.53	**−26.19**	**−14.86**
Day 14	**−19.46**	**−13.29**	**>40.0**
Day 28	**−14.98**	−5.43	**−24.19**
I_{AP}^R			
Day 1	−8.33	**32.22**	**19.31**
Day 14	**25.52**	**19.54**	**>40.0**
Day 28	**27.44**	2.51	**36.99**
I_{SM}^R			
Day 1	1.48	−1.16	0.18
Day 14	0.75	−2.34	−1.75
Day 28	−4.56	4.1	−0.16

Evidence values (in dB) for the MSL network integration, the relative AP and SM within-network integrations, as well as the relative between-network (AP/SM) integration. Differences are measured between the trained (T), untrained (U), and control (C) sequences. Significant values are marked in bold.
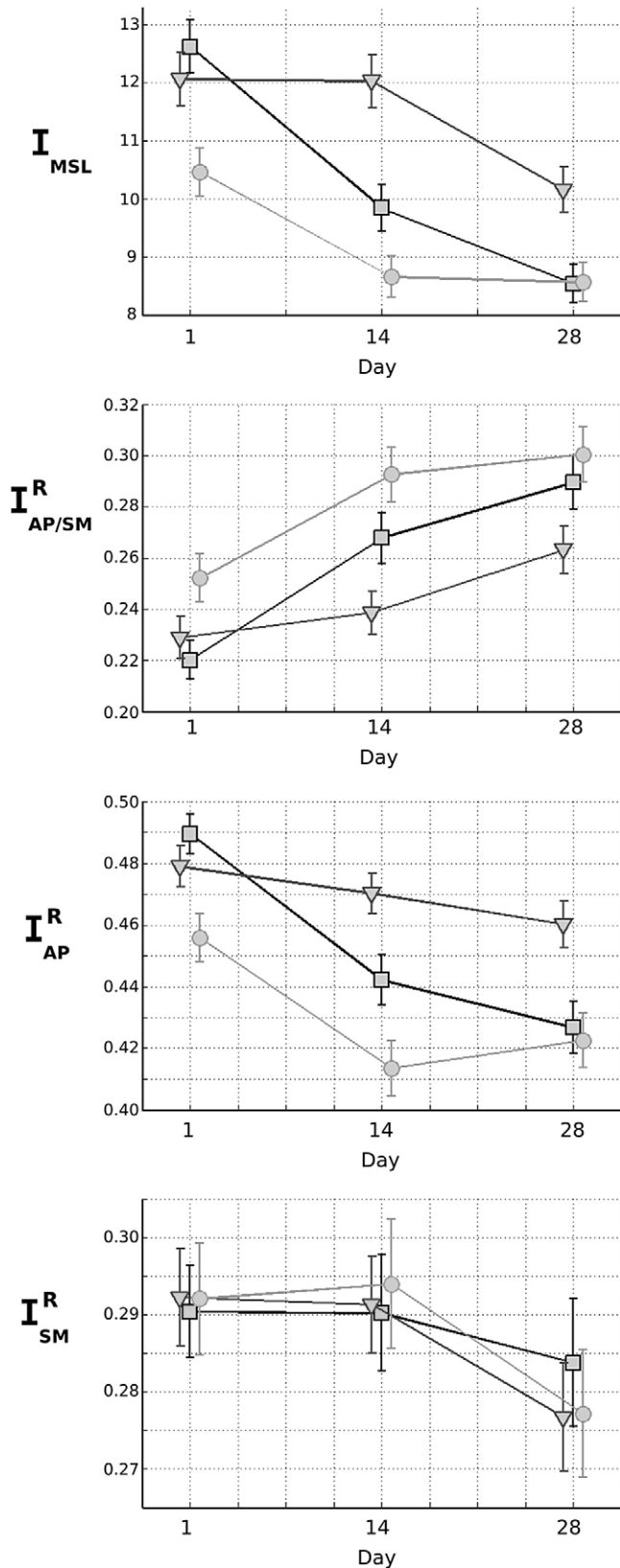
Fig. 3. Mean value ± standard deviation of MSL, AP/SM, AP, and SM integrations on days 1, 14, and 28 for the trained (squares), untrained (triangles), and control (circles) sequences.

the integration value for the C-sequence. On Day 14, all integration values differed significantly, with integration of the T-sequence being significantly lower than that of the U-sequence and higher than that of

the C-sequence. On Day 28, integrations of the T- and C-sequences did not differ ($|e| = 2.51$), and both values were smaller than the integration value of the U-sequence.

Relative SM network integration (I_{SM}^R)

No significant differences were found between the relative integration values of the T-, U-, and C-sequences in the SM network on days 1, 14, and 28.

To summarize, integration values of the new sequences (T-sequence or U-sequence) on Day 1 for the MSL network ($I_{MSL, T}$) were higher than the integration value of the simple C-sequence. Over the course of training, integration of the U-sequence remained higher than that of the C-sequence, whereas integration of the T-sequence decreased to the level of the simple C-sequence on Days 14 and 28. Therefore within the MSL network and for the T-sequence, we observed that the relative part of integration of the AP network decreased and was counterbalanced by an increase of the relative part of the integration between the AP and the SM systems.

Discussion

The objective of this paper was to study the functional connectivity of motor-related brain areas during a motor learning paradigm, over a 4-week period. The task-related functional networks were identified for each run at a group level, based on individual sICA analyses. Regions of interest were defined based on a motor skill learning model, and on the t-score distribution of the spatial maps. Functional connectivity within the MSL network was quantified using hierarchical integration, a measure that allows to summarize information exchanges between regions of a network, as well as between networks.

Selection of the regions of interest was guided by a motor skill learning model (Hikosaka et al., 2002), and applied to our data via the sICA maps. ROI selection on these maps was constrained by two anatomical atlases (Tzourio-Mazoyer et al., 2002; Yelnik et al., 2007) to remain in the framework defined by the model. We chose to apply a method based on sICA over a standard general linear model method (GLM, Friston et al. (1995)) for several reasons. First of all, sICA is a data-driven approach and therefore does not require any prior knowledge of the data (Perlbarg and Marrelec, 2008). Furthermore it is a suitable method to define regions of interest at a group level, as no prior knowledge on the spatial and temporal structure of the components is required (McKeown et al., 1998), and that task-related areas have wider spatial extents than in GLM analyses (Calhoun et al., 2001).

Hierarchical integration takes place in the framework of functional connectivity, defined as inter-regional temporal correlation between low-frequency fluctuations of the BOLD signal (Friston, 1994; Biswal et al., 1995). BOLD signal has been shown to correlate with local-field potentials, reflecting the incoming input and the local processing in a given area (Logothetis et al., 2001; Heeger and Ress, 2002). Studying functional connectivity in fMRI then gives indirect access to the average neuronal activity. Within this framework, integration was aimed at summarizing functional interactions between several regions. Indeed, when considering a large number of ROIs, correlation analyses can yield large matrices that are difficult to analyze (136 correlation coefficients with 17 ROIs). Integration summarizes temporal correlations between the time courses of several ROIs into a single value. In the simple case of a network consisting of two ROIs (Marrelec et al., 2008), it has been shown that its integration I is directly linked to the temporal correlation between ROIs $\rho : I = -\frac{1}{2}\ln(1-\rho^2)$. In this way, integration can be considered as a generalized measure of correlation between and within large-scale networks.

Among the studies that have characterized the spatial distribution of brain regions involved in motor sequence learning (Doyon et al., 2002; Lehéricy et al., 2005; Floyer-Lea and Matthews, 2005; Lehéricy et al., 2006; Tamás Kincses et al., 2008), few have tried to study functional connectivity between these regions (Rissman et al., 2004;

Sun et al., 2007). Only Sun et al. (2007) studied functional connectivity between two voxels, using a measure based on correlation. Applying hierarchical integration to study motor sequence learning allowed us to characterize the global integrative state of two networks involved in the learning task, as well as information exchanges between them, along three learning sessions.

The results show that motor sequence learning is associated with dynamic changes in the level of integration within and between the associative/premotor network and the sensorimotor network. Early learning of a complex sequence of finger movements was associated with a high level of integration of the MSL network, as compared with practice of a simple control sequence of finger movements. With practice, the functional integration of this network gradually decreased from the high level of the new complex sequence (U) to the lower level of the overlearned simple sequence (C). This decrease was mainly due to a decrease in the relative integration level of the associative/premotor network that was counterbalanced by a relative increase in the between-system integration, while the relative integration level in the sensorimotor network remained stable. Altogether, the changes observed in the spatial structure of the motor networks and their functional interaction patterns suggest that the functional connectivity associated to the trained sequence T was similar to that of the untrained sequence U at the beginning of learning, while it became similar to that of the control sequence C after learning. Trained sequences were associated with low level of within-system and high level of between-system integrations.

As previously reported, cortical and sub-cortical brain regions involved in the task differed during the early and late phases of learning. Bilateral associative/premotor regions of the cortex, the basal ganglia, and the cerebellum were involved during early but not late learning, while only sensorimotor areas of these structures, mostly contralaterally, were involved during the late phase of learning. These results are in line with numerous previous studies of motor learning, which suggested that the cortical–subcortical sensorimotor loop played a role in the long-term storage of well-learned movement sequences and that cortical–subcortical networks were involved in "automatic" movements (Ungerleider et al., 2002; Floyer-Lea and Matthews, 2004; Wu et al., 2004; Doyon and Benali, 2005; Floyer-Lea and Matthews, 2005; Lehéricy et al., 2005). In the sensorimotor cortex, increased (Hazeltine et al., 1997; Grafton et al., 1998) or, more frequently, decreased or unchanged activation was reported during short-term motor learning (Jenkins et al., 1994; Toni et al., 1998; Doyon and Ungerleider, 2002). During the late learning phase of a sequence of finger movements, increased activation was reported in the sensorimotor cortex (Karni et al., 1995; Floyer-Lea and Matthews, 2005). In our experiment, we observed two different patterns of functional integration decrease for the MSL network integration. First, there was a moderate and global decrease in integration. This decrease was not due to the learning *per se* as it was observed for the new complex sequences (U-sequences) as well as for the simple control sequence. This decrease could be linked to a global decrease in the BOLD signal between sessions that leads to a change in the measure of integration. Indeed, several studies have already reported an inter-session variability in the BOLD response (Poellinger et al., 2001; Fischer et al., 2003) or in the activation detected (Loubinoux et al., 2001; Marshall et al., 2004; Kübler et al., 2006) in brain regions involved in a task. This phenomenon can be explained by a habituation of the subject to the fMRI context, as well as to the execution of a task. It stresses the importance of having both control and novel sequences when designing a motor learning protocol over a long period of time. Second, there was a greater decrease in functional integration for the T-sequence from a level similar to the U-sequence at the beginning of learning to a lower level similar to the C-sequence after learning. This decrease was specifically related to the process of training, as it was only observed for the T-sequence and not for the two others.

We showed that motor learning was associated with a gradual decrease in the functional integration of motor-related networks over time. The overlearned sequence was associated with a low level of integration in the associative/premotor network and a relatively high level of between-system integrations, whereas the relative integration level in the sensorimotor network remained unchanged. In line with our results, previous studies have reported a greater inter- and intrahemispheric coupling within the cortical motor network as well as a greater connectivity between frontal and cortical motor regions during early learning compared with late learning in a 20-min training condition (Sun et al., 2007). Increased functional connectivity (measured with low-frequency coherence analysis) between motor regions of the two hemispheres has also been reported in a bimanual task (Rissman et al., 2004). Here, we extended these results over a 4-week training period in subjects reaching automaticity (Lehéricy et al., 2005). We further showed a dissociation between the associative/premotor network and the sensorimotor network.

In contrast to our results, an increase in functional connectivity during a 40-min training task has been observed with learning in the primary motor cortex (McNamara et al., 2007). These results are difficult to compare with ours, as we did not assess functional connectivity within the primary motor cortex itself. Given the design of our study, it was not possible to assess directly functional connectivity between digit representations in the primary motor cortex.

Our results are also partially in agreement with Hikosaka's model (Hikosaka et al., 1999, 2002). At the beginning of learning, this model postulates a high level of integration that decreases with practice in the associative/premotor network and between this network and the sensorimotor network, whereas integration in the sensorimotor network is expected to increase with practice (Hikosaka et al., 1999). Our results confirmed that integration decreases in the associative/premotor network. In contrast, functional integration in the sensorimotor network did not increase with practice. It is possible that the gradual built up of the movement sequence in the sensorimotor network does not require sustained increase in functional connectivity. Alternatively, we cannot rule out the hypothesis that functional integration may increase between digit representations within the primary motor cortex. Our results also showed that the decrease in functional connectivity was more marked for the associative/premotor network than for the integration between this network and the sensorimotor network, the relative part of which increased with practice. This suggests that interactions between these two networks may still be necessary during overlearned movements even though involvement of the regions belonging to the associative/premotor circuit is not detectable any more.

Our approach has provided a new way to quantify functional interactions within the motor network of healthy volunteers. Application to the study of movement disorders, such as dystonia, could provide relevant insight into how pathology affects the motor network.

Acknowledgments

References

Alexander, G.E., DeLong, M.R., Strick, P.L., 1986. Parallel organization of functionally segregated circuits linking basal ganglia and cortex. Annu. Rev. Neurosci. 9, 357–381.
Biswal, B., Yetkin, F. Z., Haughton, V. M., Hyde, J. S., 1995. Functional connectivity in the motor cortex of resting human brain using echo-planar MRI. Magnetic resonance in medicine: official journal of the Society of Magnetic Resonance in Medicine / Society of Magnetic Resonance in Medicine 34 (4), 537–541.
Calhoun, V.D., Adali, T., McGinty, V.B., Pekar, J.J., Watson, T.D., Pearlson, G.D., 2001. fMRI activation in a visual perception task: network of areas detected using the general linear model and independent components analysis. NeuroImage 14 (5), 1080–1088.
Doyon, J., Benali, H., 2005. Reorganization and plasticity in the adult brain during learning of motor skills. Curr. Opin. Neurobiol. 15 (2), 161–167.

Doyon, J., Ungerleider, L., 2002. Functional anatomy of motor skill learning, In: Squire, L., Schacter, D. (Eds.), Third Edition. Neuropsychology of Memory. Guilford Publications, Inc., New York, pp. 225–238.

Doyon, J., Song, A.W., Karni, A., Lalonde, F., Adams, M.M., Ungerleider, L.G., 2002. Experience-dependent changes in cerebellar contributions to motor sequence learning. Proc. Natl. Acad. Sci. U. S. A. 99 (2), 1017–1022.

Doyon, J., Bellec, P., Amsel, R., Penhune, V., Monchi, O., Carrier, J., Lehéricy, S., Benali, H., 2009. Contributions of the basal ganglia and functionally related brain structures to motor learning. Behav. Brain Res. 199 (1), 61–75.

Esposito, F., Scarabino, T., Hyvarinen, A., Himberg, J., Formisano, E., Comani, S., Tedeschi, G., Goebel, R., Seifritz, E., Salle, F.D., 2005. Independent component analysis of fMRI group studies by self-organizing clustering. NeuroImage 25 (1), 193–205.

Fischer, H., Wright, C.I., Whalen, P.J., McInerney, S.C., Shin, L.M., Rauch, S.L., 2003. Brain habituation during repeated exposure to fearful and neutral faces: a functional MRI study. Brain Res. Bull. 59 (5), 387–392.

Floyer-Lea, A., Matthews, P.M., 2004. Changing brain networks for visuomotor control with increased movement automaticity. J. Neurophysiol. 92 (4), 2405–2412.

Floyer-Lea, A., Matthews, P.M., 2005. Distinguishable brain activation networks for short- and long-term motor skill learning. J. Neurophysiol. 94 (1), 512–518.

Friston, K., Holmes, A.P., Worsley, K.J., Poline, J.B., Frith, C.D., Frackowiak, R.S., 1995. Statistical parametric maps in functional imaging: a general linear approach. Hum. Brain Mapp. 2 (4), 189–210.

Friston, K.J., 1994. Functional and effective connectivity in neuroimaging: a synthesis. Hum. Brain Mapp. 2 (1-2), 56–78.

Grafton, S.T., Hazeltine, E., Ivry, R.B., 1998. Abstract and effector-specific representations of motor sequences identified with PET. J. Neurosci. 18 (22), 9420–9428.

Hazeltine, E., Grafton, S.T., Ivry, R., 1997. Attention and stimulus characteristics determine the locus of motor-sequence encoding. A PET study. Brain 120 (Pt. 1), 123–140.

Heeger, D.J., Ress, D., 2002. What does fMRI tell us about neuronal activity. Nat. Rev., Neurosci. 3 (2), 142–151.

Hikosaka, O., Nakahara, H., Rand, M.K., Sakai, K., Lu, X., Nakamura, K., Miyachi, S., Doya, K., 1999. Parallel neural networks for learning sequential procedures. Trends Neurosci 22 (10), 464–471.

Hikosaka, O., Nakamura, K., Sakai, K., Nakahara, H., 2002. Central mechanisms of motor skill learning. Curr. Opin. Neurobiol. 12 (2), 217–222.

Hu, X., Le, T.H., Parrish, T., Erhard, P., 1995. Retrospective estimation and correction of physiological fluctuation in functional MRI. Magn. Reson. Med. 34 (2), 201–212.

Jaynes, E.T., 2003. Probability Theory: The Logic of Science. Vol. I – Principles and Elementary Applications. Cambridge University Press, Cambridge.

Jenkins, I.H., Brooks, D.J., Nixon, P.D., Frackowiak, R.S., Passingham, R.E., 1994. Motor sequence learning: a study with positron emission tomography. J. Neurosci. 14 (6), 3775–3790.

Karni, A., Meyer, G., Jezzard, P., Adams, M.M., Turner, R., Ungerleider, L.G., 1995. Functional MRI evidence for adult motor cortex plasticity during motor skill learning. Nature 377 (6545), 155–158.

Kübler, A., Dixon, V., Garavan, H., 2006. Automaticity and reestablishment of executive control—an fMRI study. J. Cogn. Neurosci. 18 (8), 1331–1342.

Lehéricy, S., Benali, H., Van de Moortele, P.-F., Pélégrini-Issac, M., Waechter, T., Ugurbil, K., Doyon, J., 2005. Distinct basal ganglia territories are engaged in early and advanced motor sequence learning. Proc. Natl. Acad. Sci. U. S. A. 102 (35), 12566–12571.

Lehéricy, S., Bardinet, E., Tremblay, L., Van de Moortele, P.-F., Pochon, J.-B., Dormont, D., Kim, D.-S., Yelnik, J., Ugurbil, K., 2006. Motor control in basal ganglia circuits using fMRI and brain atlas approaches. Cereb. Cortex 16 (2), 149–161.

Logothetis, N.K., Pauls, J., Augath, M., Trinath, T., Oeltermann, A., 2001. Neurophysiological investigation of the basis of the fMRI signal. Nature 412 (6843), 150–157.

Loubinoux, I., Carel, C., Alary, F., Boulanouar, K., Viallard, G., Manelfe, C., Rascol, O., Celsis, P., Chollet, F., 2001. Within session and between-session reproducibility of cerebral sensorimotor activation: a test–retest effect evidenced with functional magnetic resonance imaging. J. Cereb. Blood Flow Metab. 21 (5), 592–607.

Mardia, K.V., Kent, J.T., Bibby, J.M., 1979. Multivariate Analysis (Probability and Mathematical Statistics). Academic Press, London.

Marrelec, G., Krainik, A., Duffau, H., Pélégrini-Issac, M., Lehéricy, S., Doyon, J., Benali, H., 2006. Partial correlation for functional brain interactivity investigation in functional MRI. NeuroImage 32 (1), 228–237.

Marrelec, G., Bellec, P., Krainik, A., Duffau, H., Pélégrini-Issac, M., Lehéricy, S., Benali, H., Doyon, J., 2008. Regions, systems, and the brain: hierarchical measures of functional integration in fMRI. Med. Image Anal. 12 (4), 484–496.

Marshall, I., Simonotto, E., Deary, I., Maclullich, A., Ebmeier, K., Rose, E., Wardlaw, J., Goddard, N., Chappell, F., 2004. Repeatability of motor and working-memory tasks in healthy older volunteers: assessment at functional MR imaging. Radiology 233 (3), 868–877.

McKeown, M.J., Makeig, S., Brown, G.G., Jung, T.P., Kindermann, S.S., Bell, A.J., Sejnowski, T.J., 1998. Analysis of fMRI data by blind separation into independent spatial components. Hum. Brain Mapp. 6 (3), 160–188.

McNamara, A., Tegenthoff, M., Dinse, H., B chel, C., Binkofski, F., Ragert, P., 2007. Increased functional connectivity is crucial for learning novel muscle synergies. NeuroImage 35 (3), 1211–1218.

Perlbarg, V., Marrelec, G., 2008. Contribution of exploratory methods to the investigation of extended large-scale brain networks in functional MRI: methodologies, results, and challenges. Int. J. Biomed. Imag. 14. doi:10.1155/2008/218519.

Perlbarg, V., Marrelec, G., Doyon, J., Pélégrini-Issac, M., Lehéricy, S., Benali, H., 2008. NEDICA: detection of group functional networks in FMRI using spatial independent component analysis. Proceedings of the 5th IEEE International Symposium on Biomedical Imaging: From Nano to Macro, 2008. ISBI 2008., 1247–1250.

Poellinger, A., Thomas, R., Lio, P., Lee, A., Makris, N., Rosen, B.R., Kwong, K.K., 2001. Activation and habituation in olfaction—an fMRI study. NeuroImage 13 (4), 547–560.

Rissman, J., Gazzaley, A., D'Esposito, M., 2004. Measuring functional connectivity during distinct stages of a cognitive task. NeuroImage 23 (2), 752–763.

Romanelli, P., Esposito, V., Schaal, D.W., Heit, G., 2005. Somatotopy in the basal ganglia: experimental and clinical evidence for segregated sensorimotor channels. Brain Res. Rev. 48 (1), 112–128.

Shannon, C., 1948. A mathematical theory of communication. Bell Syst. Tech. J. 27, 379–423.

Sun, F.T., Miller, L.M., Rao, A.A., D'Esposito, M., 2007. Functional connectivity of cortical networks involved in bimanual motor sequence learning. Cereb. Cortex 17 (5), 1227–1234.

Tamá s Kincses, Z., Johansen-Berg, H., Tomassini, V., Bosnell, R., Matthews, P.M., Beckmann, C.F., 2008. Model-free characterization of brain functional networks for motor sequence learning using fMRI. NeuroImage 39 (4), 1950–1958.

Toni, I., Krams, M., Turner, R., Passingham, R., 1998. The time course of changes during motor sequence learning: a wholebrain fMRI study. NeuroImage 8 (1), 50–61.

Tononi, G., Sporns, O., Edelman, G.M., 1994. A measure for brain complexity: relating functional segregation and integration in the nervous system. Proc. Natl. Acad. Sci. U. S. A. 91 (11), 5033–5037.

Tzourio-Mazoyer, N., Landeau, B., Papathanassiou, D., Crivello, F., Etard, O., Delcroix, N., Mazoyer, B., Joliot, M., 2002. Automated anatomical labeling of activations in SPM using a macroscopic anatomical parcellation of the MNI MRI single subject brain. NeuroImage 15 (1), 273–289.

Ungerleider, L., Doyon, J., Karni, A., 2002. Imaging brain plasticity during motor skill learning. Neurobiol. Learn. Mem. 78 (3), 553–564.

Varela, F., Lachaux, J.P., Rodriguez, E., Martinerie, J., 2001. The brainweb: phase synchronization and large-scale integration. Nat. Rev. Neurosci. 2 (4), 229–239.

Watanabe, S., 1960. Information theoretical analysis of multivariate correlation. IBM J. Res. Dev. 4, 66–82.

Wu, T., Kansaku, K., Hallett, M., 2004. How self-initiated memorized movements become automatic: a functional MRI study. J. Neurophysiol. 91 (4), 1690–1698.

Yelnik, J., Bardinet, E., Dormont, D., Malandain, G., Ourselin, S., Tand é, D., Karachi, C., Ayache, N., Cornu, P., Agid, Y., 2007. A three-dimensional, histological and deformable atlas of the human basal ganglia. I. Atlas construction based on immunohistochemical and MRI data. NeuroImage 34 (2), 618–638.